GA–A22803

ELECTRON CYCLOTRON HEATING EXPERIMENTS ON THE DIII–D TOKAMAK

by

R. PRATER, M.E. AUSTIN, S. BERNABEI,
R.W. CALLIS, J.S. deGRASSIE, Y.R. LIN-LIU,
J.M. LOHR, T.C. LUCE, M. MURAKAMI, C.C. PETTY,
R.I. PINSKER, D. PONCE, and M. ZERBINI

JANUARY 1998

GA–A22803

ELECTRON CYCLOTRON HEATING EXPERIMENTS ON THE DIII–D TOKAMAK

by

R. PRATER, M.E. AUSTIN,[1] S. BERNABEI,[2]
R.W. CALLIS, J.S. deGRASSIE, Y.R. LIN-LIU,
J.M. LOHR, T.C. LUCE, M. MURAKAMI,[3] C.C. PETTY,
R.I. PINSKER, D. PONCE, and M. ZERBINI[4]

This is a preprint of a paper presented at the Second Europhysics Topical Conference on RF Heating and Current Drive of Fusion Devices, January 20–23, 1998, Brussels, Belgium, and to be printed in the *Proceedings.*

Work supported by U.S. Department of Energy under
Contracts DE-AC03-89ER51115, DE-FG05-96ER54373,
DE-AC02-76CH03073, and DE-AC05-96OR22464.

[1]University of Texas
[2]Princeton Plasma Physics Laboratory
[3]Oak Ridge National Laboratory
[4]ENEA CRE, Frascati

GENERAL ATOMICS PROJECT 3466
JANUARY 1998

Electron Cyclotron Heating Experiments on the DIII-D Tokamak

R. Prater, M.E. Austin,[1] S. Bernabei,[2] R.W. Callis, J.S. deGrassie, Y.R. Lin-Liu, J.M. Lohr, T.C. Luce, M. Murakami,[3] C.C. Petty, R.I. Pinsker, D. Ponce, and M. Zerbini[4]

General Atomics, San Diego, California 92186-5608, U.S.A.

Abstract. Initial experiments on heating and current drive using second harmonic electron cyclotron heating (ECH) are being performed on the DIII-D tokamak using the new 110 GHz ECH system. Modulation of the ECH power in the frequency range 50 to 300 Hz and detection of the temperature perturbation by ECE diagnostics is used to validate the location of the heating. This technique also determines an upper bound on the width of the deposition profile. Analysis of electron cyclotron current drive indicates that up to 0.17 MA of central current is driven, resulting in a negative loop voltage near the axis.

Initial experiments have been performed on the DIII-D tokamak using up to 1.1 MW of 110 GHz electron cyclotron heating (ECH) power from two gyrotrons. The frequency corresponds to the second harmonic of the electron cyclotron frequency. The initial ECH system which used a 1 MW Gycom gyrotron has been described in Ref. 1, and since that time an additional system using a 1 MW CPI gyrotron has been completed. In these experiments the Gycom gyrotron was operated for 2 s pulses at 0.8 MW and the CPI gyrotron for 1 s at 0.7 MW. The pulse length of both gyrotrons is known to be limited by their microwave windows. Each gyrotron has an internal mode converter which generates a ‘‘flattened Gaussian’’ beam which is coupled to the HE_{11} mode of a circular waveguide via a pair of phase correcting mirrors. The transmission line is windowless evacuated corrugated waveguide of relatively small diameter, 31.75 mm, which has operated with excellent reliability in extensive operation. The power is launched into the DIII–D vacuum vessel as two narrow beams which theoretically, in the far-field region, expand with a half-angle of 2.9 deg. This implies a diameter of 56 mm for the contour of 1/e in power (a contour including 63% of the incident power) at a ray path length of 800 mm, the approximate distance from the launching mirror to the center of the plasma along a ray path. The launching mirror has a fixed inclination in the toroidal direction of 19 deg in these experiments, and the mirror assembly can be rotated about a horizontal axis between discharges, thereby steering the beam in the vertical direction. For a toroidal field such that the resonance goes through the plasma center and a steering angle which directs the beam to the plasma center, the included angle at the resonance of the intersection of the beam with the magnetic field is about 52 deg. This is a strong toroidal inclination, and the product of the electron density and the electron temperature must be above about 2.5×10^{19} keV/m^3 to obtain sufficient wave absorption for current drive. The polarization of the launched wave is calculated to be a nearly pure X–mode.

[1]University of Texas, Austin, Texas, U.S.A.; [2]Princeton Plasma Physics Laboratory, Princeton, New Jersey, U.S.A.; [3]Oak Ridge National Laboratory, Oak Ridge, Tennessee, U.S.A; [4]ENEA CRE, Frascati, Italy.

Plasma Heating Characteristics

The location of the deposition of the power in the plasma can be determined by modulating the ECH and detecting the modulation in the electron temperature at the corresponding frequency. Figure 1(a) shows the vacuum ray paths through the plasma for five angles of the steering mirror used in the experiment. The ray paths shown are straight lines in three dimensional space projected onto a plane of constant azimuth. The experiments were performed at densities below 1×10^{19} m^{-3} in order to maximize the electron temperature response. Electron cyclotron emission provides a calibrated measure of flux-surface averaged electron temperature with good sensitivity and time response. A curve fit to the amplitude signals from the 32 channels of the radiometer for each mirror position is shown in Fig. 1(b). Qualitatively, the agreement between the rays shown in Fig. 1(a) and the responses shown in Fig. 1(b) is good, with the peak in the response corresponding to the first crossing of the resonance by the ray in each case. In some cases, a ray may cross the resonance well off-axis where the temperature is low and the absorption is poor. Its second transit of the resonance may be much closer to the plasma center where the absorption rate is much larger and the plasma volume is smaller. This can cause a second peak in the response, as for mirror position 4 in Fig. 1(b). This effect can also be due to absorption of the relatively small O–mode component of the wave, which is very poorly absorbed off-axis but is moderately absorbed on-axis.

The width of the response curves in Fig. 1(b) should not be taken to be the width of the deposition profile. Transport on the time scale of the modulation period can significantly broaden the response profile [2], which can be seen from the phase of the T_e response relative to the heating phase. As the modulation frequency is increased, the temperature response curves more closely approach the deposition profile, but the amplitude of the response also decreases. The signal-to-noise ratio therefore places an upper limit on the modulation frequency which is below the frequency needed for direct determination of the deposition profile for our systems.

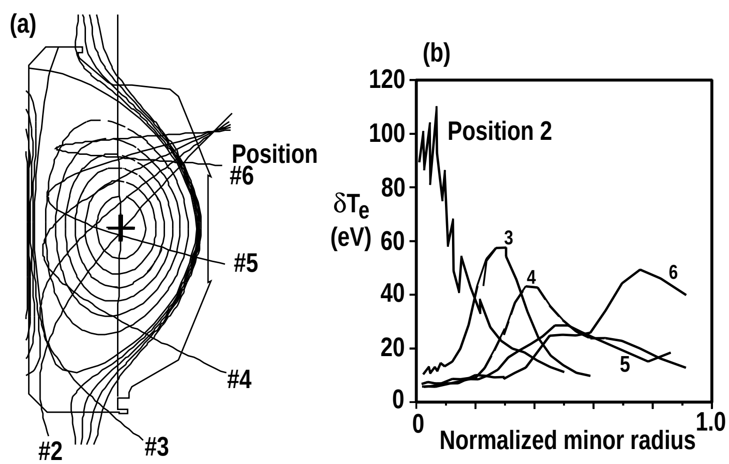

Fig. 1. (a) ECH ray paths through the plasma for five settings of the vertical steering mirror. (b) Amplitude of the electron temperature response as a function of the plasma minor radius, from ECE measurements. The modulation frequency is 100 Hz.

Electron Cyclotron Current Drive

Experiments on ECCD were performed in discharges in which early neutral beams are applied in order to suppress sawteeth during the current drive phase. The neutral beam heating also raises the electron temperature which facilitates the full absorption of the waves on the launcher side of the resonance and provides signal for the motional Stark effect diagnostic. Since sawteeth are absent, the profile of electron cyclotron driven current can be determined even in the presence of back-induced Ohmic currents which tend to mask the driven current for short time scales . The technique [3] uses a time sequence of reconstructed equilibria to determine the equilibrium current density and local electric field E (from the time derivative of the flux). The EC-driven current density j_{EC} is found from the equation $j_{EC} = j_{tot} - j_{oh} - j_{NB} - j_{BS}$, where $j_{oh} = \sigma E$ and σ is the local conductivity determined from measurements of the plasma parameters. The neutral beam driven current j_{NB} and the bootstrap current j_{BS} are subtracted by comparing discharges with and without ECH. Under the assumption, which must yet be validated, that the ECH is a small perturbation (for $P_{ECH} \ll P_{NB}$) which does not much affect j_{NB} and j_{BS}, the current density j_{EC} can be estimated.

EC driven currents up to 170 kA have been found in this manner. Figure 2 shows calculations for a pair of such discharges, one with and one without ECH. The orientation of the ECH beam is such as to drive co-current near the plasma axis. The total current density for the two discharges from EFIT calculations is shown in Fig. 2(a), and the local electric field is shown in Fig. 2(b). Note that while the difference in loop voltage at the edge is small, the difference near the center of the discharge is large, with the central electric field reversing sign near the axis. This is an indication that the driven current exceeds the equilibrium current, and the electric field adjusts by Lenz's law to conserve the flux. Subtracting the Ohmic current density from the total current density for each discharge gives the noninductive current density, shown in Fig. 2(c). Integrating the difference, again assuming that the NB and bootstrap currents are unaffected by the ECH, gives the total current, shown in Fig. 2(d). The 170 kA of driven current is in good

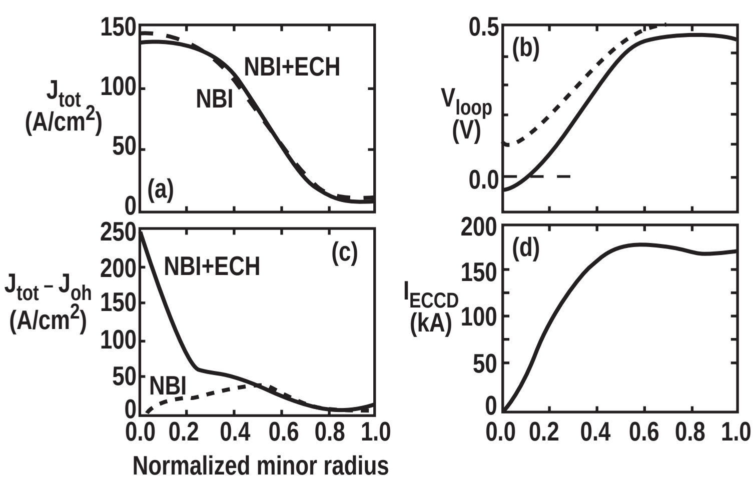

Fig. 2. Profiles for two discharges, one with 0.82 MW of ECH (solid line, discharge 94188) and one without ECH (dashed line). (a) total current density, (b) loop voltage, c) noninductive current density, and (d) integrated current. The NB power is 2.8 MW, the density is 1×10^{19} m^{-3}, and the plasma current is 1.0 MA.

agreement with calculations using the TORAY ray tracing code, and it represents a figure of merit $\gamma = 0.35\times10^{19}$ A/W m^2.

This central EC current drive can affect the evolution of the current profile, as shown in Fig. 3. This figure shows two discharges, with and without ECCD. Figure 3(b) shows that the central safety factor q(0) falls much more rapidly in the presence of co-ECCD. If the only effect of the ECH were electron heating, the decrease in q(0) should be slower, not faster, than the NB-only case due to increased electrical conductivity. The evolution of the current density demonstrated by the q(0) behavior is corroborated by the calculations of the internal inductance [Fig. 3(c)], which rises significantly faster in the ECH case, as expected for increasing central current density. Figure 3(d) shows that the central back-EMF is still large, indicating that much larger changes in the current profile can be supported by this level of ECCD.

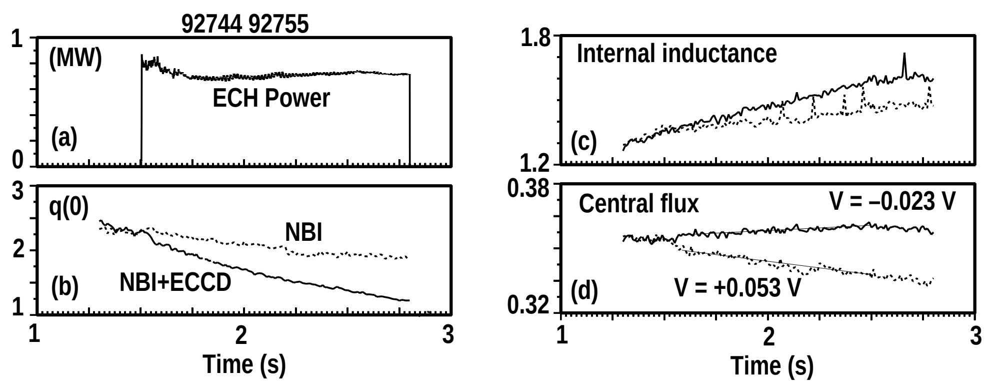

Fig. 3. Evolution of two discharges, one with ECH power (solid line) and one without (dashed line). (a) ECH power, (b) central safety factor, (c) internal inductance, and (d) central flux. The NB power is 2.6 MW, the density is 1×10^{19} m^{-3}, the plasma current is 0.6 MA, and the toroidal field is 2.0 T.

This work shows that effective electron heating is taking place at the expected location. Central current drive in rough agreement with calculations is observed, and this driven current can affect the evolution of the current density profile. A key task for the future is the test of off-axis current drive and its application to advanced tokamak discharges in DIII–D.

This is a report of work sponsored by the U.S. Department of Energy under Contracts DE-AC03-89ER51114, DE-FG05-96ER54373, DE-AC02-76CH03073, and DE-AC05-96OR22464.

References

[1] R.W. Callis, J. Lohr, R.C. O'Neill, *et al.*, in Radio Frequency Power in Plasmas, 12th Topical Conference, Savannah, 1997, AIP Conference Proceedings 403 (AIP, 1997), p. 197.

[2] F. Leuterer, H. Brinkschulte, F. Monaco, *et al.*, 23rd EPS Conference on Controlled Fusion and Plasma Physics, Kiev, 1996, Vol. 2, p. 871.

[3] C.B. Forest *et al.*, Phys. Rev. Lett. **73**, 2444 (1994).